

Photoinduced Electron Transfer in Ruthenium Bipyridyl Complexes: Evidence for the Existence of a Cage with Molecular Oxygen

Eylon Yavin,^{†,§} Lev Weiner,^{*,‡} Rina Arad-Yellin,[†] and Abraham Shanzer^{*,†}

Department of Organic Chemistry and Department of Chemical Research Support,
Weizmann Institute of Science, Rehovot 76100, Israel

Received: April 22, 2004; In Final Form: July 30, 2004

Ruthenium complexes with three bipyridyl ligands, one of which is modified by attaching one or two hydroxamic acids groups (**Ru-1** and **Ru-2**, respectively), were synthesized. Using EPR spectroscopy, we have found that photoexcitation leads to formation of nitroxyl radicals. The nitroxyl radical concentration in **Ru-2** increased dramatically in the presence of spin traps DMPO (5,5'-dimethyl-1-pyrroline-*N*-oxide) and PBN (*N*-tert-butyl- α -phenylnitron) characterized by strong affinity to superoxide radicals. We have attributed this behavior to the formation of a cage complex between **Ru-2** and the superoxide radical. This paper concerns the study of cages formed between ruthenium complexes and molecular oxygen and the effect of functional groups attached to modified bipyridyl ligands on cage formation. The complex between **Ru-2** and O₂ was formed in the ground state, probably with participation of the hydroxamic acid groups. The equilibrium constant of this complex was determined by EPR as $K_{\text{eq}} \sim 3 \text{ M}^{-1}$. The formation of the **Ru-2**-O₂ complex is supported by the temperature-dependent rate of appearance of the EPR signal in the presence of PBN. Additional evidence comes from observation of paramagnetic shifts of the peaks in the ¹H NMR spectrum of specific aromatic protons in the substituted bipyridyl ring upon exposure to O₂. Similar shifts were observed in the spectrum of **Os-2**, with osmium replacing ruthenium. Model compounds with functional groups that replace the hydroxamic acid or compounds without the metal center, but with the two hydroxamic acids, were synthesized. No shifts in the ¹H NMR spectra of these derivatives were observed in the presence of O₂. These results lead to the conclusion that both metal ions, Ru(II) or Os(II), and hydroxamic acid groups are essential components for the formation of the oxygen cage.

Introduction

Many efforts have been made to use the powerful oxidation potential of photogenerated ruthenium(III) polypyridyl complexes to catalyze oxidation of water,^{1–7} DNA, and RNA.^{8–15} Ruthenium complexes were also incorporated into specific sites of proteins and nucleic acids and were used to study photoinduced electron-transfer processes in these biopolymeric systems.^{8,16–28}

Quenching the excited states of ruthenium tris bipyridine complexes by molecular oxygen leads to either an energy-transfer process that yields singlet oxygen and the Ru(II) ion in its ground state (Scheme 1B) or an electron-transfer process that yields superoxide radicals and Ru(III) ions (Scheme 1A). Using transient absorption spectroscopy of Ru(II), Zhang and Rodgers²⁹ have suggested that a 'cage' complex consisting of Ru(III) and superoxide radical is formed when the electron transfer is the process of choice. For neutral pH, the 'cage' complex is not liberated; that is, the electron-transfer process has a quantum yield of zero. In acidic conditions (3 N D₂SO₄), the superoxide radical is released from the cage and Ru(III) is formed, with a quantum yield of 0.55.²⁹

Hydroxamic acids are bidentate ligands found in many natural products, especially in those that bind ferric ions. In neutral solutions, the hydroxamic acid can be oxidized by hydroxyl and superoxide radicals that yield nitroxyl radicals.^{30,31}

The synthesis and photochemical behavior of a ruthenium tris bipyridine complex where one of its bipyridyl ligands was modified with two arms, each bearing a hydroxamic acid group (**Ru-2**, Scheme 1C),³² were reported previously. The electron- and energy-transfer processes in the presence of molecular oxygen were detected by EPR, following the kinetics of the formation of nitroxyl radicals formed on the hydroxamic acid side chain. In the absence of O₂, nitroxyl radical did not form, whereas in the presence of superoxide dismutase (SOD) radical formation was enhanced.³² Thus, we have suggested that **Ru-2** forms a genuine cage complex with a superoxide radical, which can be released by adding molecules such as PBN and DMPO with high affinity for superoxide radicals and that act as spin traps. Consequently, the electron-transfer process, that is otherwise dormant, is activated and leads to Ru(III) generation (Scheme 1A).

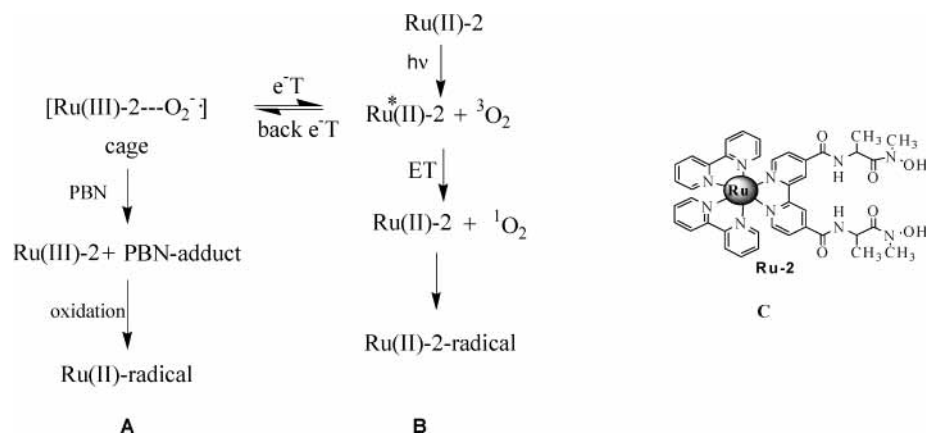
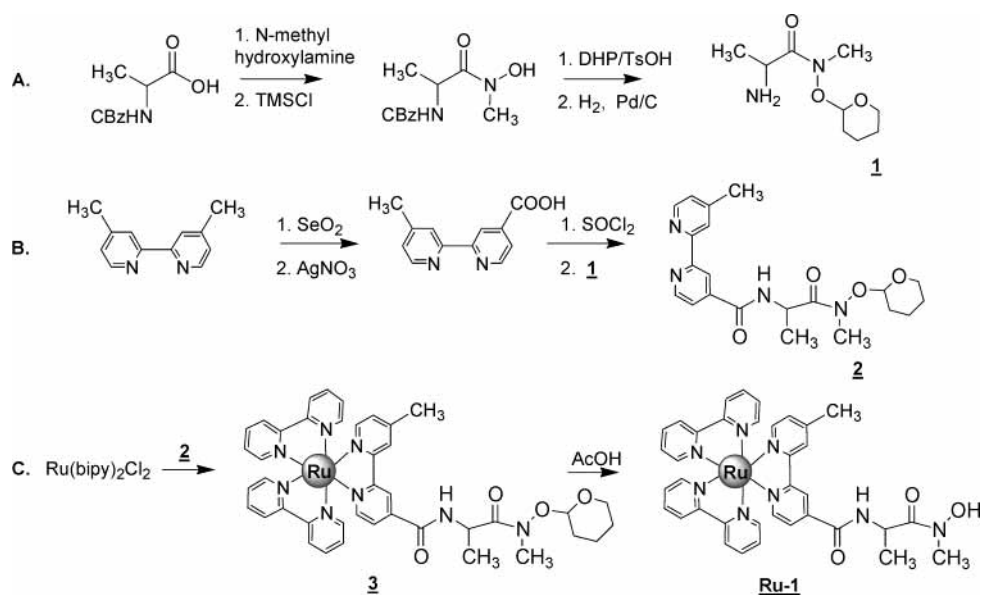
To assess the role of the different components in **Ru-2**'s affinity for molecular oxygen, we synthesized an analogous ruthenium complex **Ru-1** (Scheme 2) that has a single hydroxamic acid group on one of the bipyridyl ligands, and compared the nitroxyl radicals' formation by **Ru-2** and **Ru-1**. Two hydroxamic acid groups were indispensable for stabilization of the cage complex formed between ruthenium in its trivalent oxidation state and superoxide radical. The affinity for O₂ (K_{cage}) was estimated from the EPR data.

* To whom correspondence should be addressed: abraham.shanzer@weizmann.ac.il; Phone: 972-8-9343954; Fax: 972-8-9432917. lev.weiner@weizmann.ac.il; Phone: 972-8-9343410; Fax: 972-8-9346017.

[§] California Institute of Technology, Department of Chemistry & Chemical Eng., Pasadena, CA 91125.

[†] Department of Organic Chemistry, Weizmann Institute of Science.

[‡] Department of Chemical Research Support, Weizmann Institute of Science.

SCHEME 1: Photoinduced Electron (A) and Energy (B) Transfer Processes in the Ru-2 Complex (C) in the Presence of O₂**SCHEME 2: Synthesis of Ru-1**

Oxygen is a paramagnetic molecule that can induce chemical shifts in the NMR signals of magnetically active atoms that are in close contact with it³³ and is highly solvable in hydrophobic solvents. In general,³⁴ and in the interior of cell membranes in particular, this technique was used for probing the structure of certain membrane proteins.³⁵ We used NMR for tracking the interactions between **Ru-2** and molecular oxygen and observed changes in chemical shifts of selective protons of the modified bipyridyl ring in the presence of O₂. This fact strengthened the

conclusion based on the EPR data. Model compounds that lack the metal center and either one or two of the hydroxamic acid groups did not reveal any significant shifts in the ¹H NMR signals in the presence of O₂. This observation suggests that the metal center and hydroxamic acids groups can be crucial for the formation of the cage. The EPR and NMR data and the study of various model compounds taken together, we suggest that an oxygen cage is formed between **Ru-2** and molecular oxygen (Figure 1).

Experimental Section

Instrumentation. The ¹H NMR spectra were measured on an Avance DPX-400 MHz or DPX-250 MHz spectrometer (Bruker) using the solvent deuterium signal as an internal reference. All *J* values are given in Hertz. The IR spectra were recorded on a Protégé 460 FTIR spectrometer. The UV-vis spectra were measured with a Hewlett-Packard model 8450A diode array spectrophotometer. MS-ES was performed at the Weizmann Institute (Rehovot). Flash chromatography was performed using Merck 230–400 mesh silica gel. Thin layer chromatography (TLC) on 60 F-254 silica gel was visualized by UV light and by one or more of the following reagents: ninhydrin, basic KMnO₄ solution, or iodine, or by FeCl₃ in MeOH. The X-band EPR spectra were recorded on an Electron

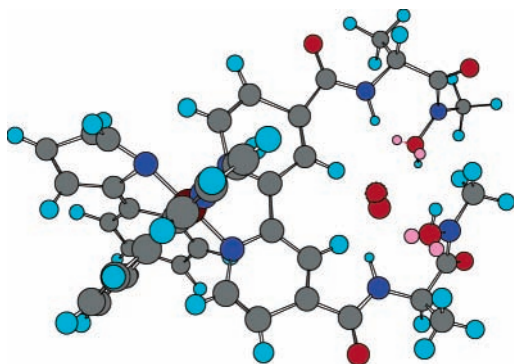


Figure 1. Schematic view (chem3D) of the cage formed between **Ru-2** and O₂ (red = oxygen, blue = nitrogen, gray = carbon, and light blue = hydrogen).

Spin Resonance ER 200D-SRC spectrometer (Bruker) at room temperature and at elevated temperatures.

Chemicals. Chemicals and reagents were purchased from Sigma. The *cis*-dichloro bis(2,2'-bipyridine) ruthenium(II) dihydrate was purchased from STREM chemicals. Dichloromethane (DCM) was dried by passing the solvent through a basic alumina column. Tetrahydrofuran (THF) was distilled from Na under argon. Double distilled water and spectroscopic grade CH₃CN were used for EPR experiments.

The spin traps (DMPO (5,5'-dimethyl-1-pyrroline-*N*-oxide) and PBN (*N*-*tert*-butyl- α -phenylnitron)) were purchased from Sigma and purified as described before.³²

EPR Experiments. The EPR experiments were carried out in CH₃CN/H₂O (93:7) solutions. A quartz flat cell of 70 μ L was used in all experiments when the recording was accompanied by illumination. A 150 W lamp (Schott model KL 1500 LCD) adjusted with different filters was used as a light source. The ruthenium complexes were illuminated using a blue filter (380–500 nm). The osmium complex was illuminated without a filter. The temperature was adjusted by a temperature unit control (Eurotherm, B-VT 2000) with accuracy of ± 1 K. The stable nitroxyl radical TEMPO was used as a standard. Double integration of EPR peaks was used for estimating the nitroxyl radical concentration.

The abbreviations for the NMR spectra are as follows: bipy = bipyridyl, s-bipy = substituted bipyridyl, *ov* = overlapping proton peaks, *d* = doublet, *s* = singlet, and *t* = triplet.

The synthetic protocol of **Ru-2** was already published.³² The **Ru-1** was synthesized starting from 2,2'-bipyridyl-4-methyl-4'-carboxylic acid³⁶ following a similar protocol as described in Scheme 2. The acid was suspended in SOCl₂ and refluxed for 5 h, followed by removal of the solvent. The acyl chloride was dissolved in dry THF, and triethylamine (415 μ L, 3 mmol) was added followed by 2-amino-*N*-methyl-*N*-(tetrahydropyran)propioic acid (**1**)³⁷ (2 mmol) dissolved in THF. The pH was adjusted to 8 by triethylamine, and the reaction mixture was left to stir overnight at room temperature. The solvent was removed, and the crude material was purified by column chromatography, using a mixture of ethyl acetate/MeOH/25% ammonia solution (97.5:2:0.5) as eluent. The product **2** (310 mg, 0.78 mmol) was obtained in 65% yield.

¹H NMR (250 MHz, CDCl₃) δ = 8.78 (*d*, *J* = 2.5 Hz, 1H, bipy 3), 8.67 (*m*, 1H, bipy 3), 8.53 (*m*, 1H, bipy 6), 8.22 (*m*, 1H, bipy 5), 7.73 (*m*, 1H, bipy 6'), 7.42 (*br*, 1H, *NH*), 7.15 (*m*, 1H, bipy 5'), 5.15–5.8 (*br*, 1H of THP *CHO*), 5.10 (*m*, 1H, *NHCH*CH₃), 4.05 and 3.65 (*m*, 2H of THP *OCH*₂), 3.40 (*s*, 3H, *NCH*₃), 2.43 (*s*, 3H, bipy-*CH*₃), 1.84 and 1.66 (*br*, 6H, THP *CHCH*₂*CH*₂*CH*₂), 1.48 (*m*, 3H, *CHCH*₃). IR (CHCl₃): ν = 1640 cm⁻¹ (*CONO*).

The **Ru-1** was obtained by removal of the protecting group from **3**. It was done by heating **3** (308 mg, 0.33 mmol) for 1 h to 60 °C in a 50% acetic acid solution. The solvent was evaporated; the residue was dissolved in a minimum amount of MeOH and dropped into a cold ether solution. Complete precipitation was obtained after the solution had been left in the refrigerator for the night. It was filtered and washed with diethyl ether. **Ru-1** (271 mg) was obtained in 97% yield.

¹H NMR (400 MHz, MeOH-*d*₄) δ = 9.07 (*s*, 1H, s-bipy 3), 8.66–8.69 (*ov*, 5H, bipy 3,3' and s-bipy 3'), 8.11 (*m*, 4H, bipy 4,4'), 7.93 (*d*, *J* = 6 Hz, 1H, s-bipy 6), 7.78–7.83 (*ov*, 5H, bipy 6,6' and s-bipy 5), 7.63 (*d*, *J* = 6 Hz, 1H, s-bipy 6'), 7.48 (*m*, 4H, bipy 5,5'), 7.36 (*m*, 1H, s-bipy 5'), 5.18 (*q*, *J* = 7 Hz, 1H, *NHCH*), 3.23 (*s*, 3H, *NCH*₃), 2.59 (*s*, 3H, bipy-*CH*₃), 1.47 (*dd*, *J* = 7.2, 1.6 Hz, 3H, *NHCHCH*₃). IR (KBr): ν = 1635

cm⁻¹ (*CONO*). UV λ_{\max} (ϵ) = 289 (47 200) and 477 (8800) nm. MS-ES *m/z* = 851 [M-H]¹⁺.

The ruthenium complex with protected hydroxamic acids **3** was prepared by refluxing an 80% ethanolic solution of **2** (230 mg, 0.577 mmol) and Ru(bipy)₂Cl₂·6H₂O (355 mg, 0.60 mmol) for 4 h under argon. The solvent was removed, and the product was purified by column chromatography eluting with a solution containing CH₃CN/*n*-BuOH/0.4 M KNO₃ (9:0.5:0.5). The Ru complex **3** (308 mg) was obtained in 57% yield.

¹H NMR (250 MHz, MeOH-*d*₄) δ = 9.08 (*s*, 1H, s-bipy 3), 8.64–8.71 (*ov*, 5H, bipy 3,3' and s-bipy 3'), 8.12 (*t*, *J* = 8 Hz, 4H, bipy 4,4'), 7.95 (*d*, *J* = 6 Hz, 1H, s-bipy 6), 7.78–7.85 (*ov*, 5H, bipy 6,6' and s-bipy 5), 7.64 (*d*, *J* = 6 Hz, 1H, s-bipy 6'), 7.48 (*m*, 4H, bipy 5,5'), 7.37 (*m*, 1H, s-bipy 5'), 5.35 (*br*, 1H, THP, *OCH*), 4.95 (*q*, *J* = 7 Hz, 1H, *NHCH*), 4.06 and 3.66 (*m*, 2H of THP, *OCH*₂), 3.32 and 3.38 (*s*, 3H, *NCH*₃), 2.58 and 2.60 (*s*, 3H, bipy-*CH*₃), 1.65–1.84 (*ov*, 6H, THP, *OCHCH*₂*CH*₂*CH*₂), 1.50 (*d*, *J* = 8 Hz, 3H, *NHCHCH*₃). IR (KBr) ν = 1640 cm⁻¹ (*CONO*).

Os(bipy)₂Cl₂. The Os(bipy)₂Cl₂ was prepared according to literature protocol³⁸ and was refluxed with **1** in ethanolic solution to yield compound **Os-1**, which was converted to **Os-2** as described for **Ru-2**.³²

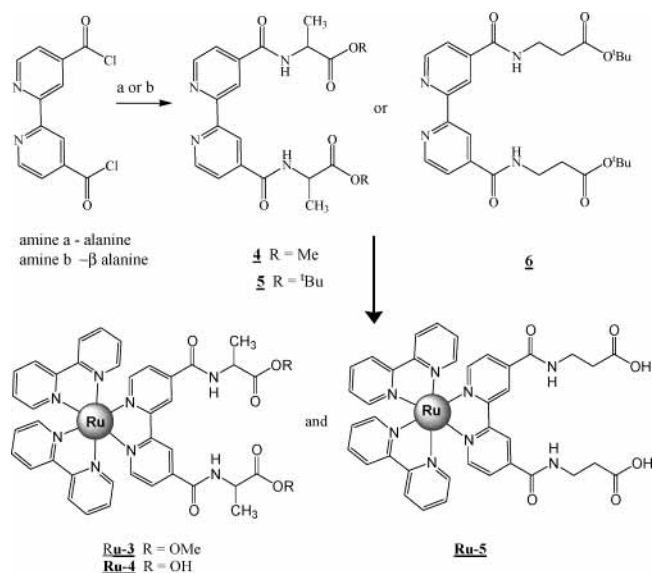
Os-1. ¹H NMR (250 MHz, MeOH-*d*₄) δ = 9.16 (*m*, 2H, s-bipy 3,3'), 8.68 (*m*, 4H, bipy 3,3'), 8.00–7.92 (*m*, 6H, bipy 4,4' and s-bipy 5,5'), 7.71 (*m*, 6H, bipy 6,6' and s-bipy 6,6'), 7.45 (*m*, 4H, bipy 5,5'), 5.34 (*br*, 2H, THP), 4.96 and 5.05 (*br*, 2H, *NHCH*×2), 4.00 and 3.67 (*m*, 4H of THP), 3.34–3.36 (*ov*, 6H, *NCH*₃×2), 1.67–1.82 (*ov*, 12H, THP), 1.44 (*m*, 6H, *CHCH*₃×2). IR (KBr): ν 1640 cm⁻¹ (*CONO*). MS-ES *m/z* = 558.6 [M]²⁺.

Os-2. ¹H NMR (250 MHz, MeOH-*d*₄) δ = 9.19 (*s*, 2H, s-bipy 3,3'), 8.70 (*m*, 4H, bipy 3,3'), 7.95 (*m*, 6H, bipy 4,4' and s-bipy 5,5'), 7.70 (*m*, 6H, bipy 6,6' and s-bipy 6,6'), 7.41 (*m*, 4H, bipy 5,5'), 5.18 (*m*, 2H, *NHCH*×2), 3.23 (*s*, 6H, *NCH*₃×2), 1.47 (*d*, *J* = 7 Hz, 6H, *CHCH*₃×2). IR (KBr): ν = 1635 cm⁻¹ (*CONO*). UV λ_{\max} (ϵ) = 290 (20 885) and 493 (4350) nm. MS-ES *m/z* = 474.5 [M]²⁺.

Phen-1. The 4-carbomethoxy-benzyl bromide (540 mg, 2.35 mmol), prepared from the acid,³⁹ and triphenylphosphine (667 mg, 2.58 mmol) were dissolved in toluene (8 mL) under an inert atmosphere (argon), and the solution was warmed to 80 °C for 5 h. After cooling to RT the solution was cooled in an ice bath and the resulting precipitate was filtered, washed with toluene, and dried under high vacuum to afford 4-carbomethoxy-benzyltriphenylphosphonium bromide (828 mg, 72% yield) as a white solid. To this were added methyl-4-formylbenzoate (2.02 mmol) and sodium methoxide⁴⁰ to yield the corresponding stilbene derivative. The *trans*-stilbene isomer (200 mg) precipitated by cooling, and the *cis* isomer (100 mg) was recovered from the mother liqueur and was purified by column chromatography. The yield of both isomers was 60%.

Irradiation of a benzene solution of a mixture of *cis*- and *trans*-dimethyl 4, 4'-stilbene-dicarboxylate (300 mg) yielded dimethyl 3,6-phenanthrenedicarboxylate⁴¹ (163 mg, 0.55 mmol in 55% yield). It was further hydrolyzed to the corresponding 3, 6-phenanthrene dicarboxylic acid⁴² and was further converted to **Phen-1** in a protocol similar to that described for **Ru-2**.³² Purification was done by column chromatography using 0–4% MeOH in CHCl₃ as eluent. The product **Phen-1** (139 mg) was obtained in 86% yield.

¹H NMR (250 MHz, CDCl₃) δ = 9.37 (*s*, 2H), 8.08 (*m*, 2H), 7.92 (*m*, 2H), 7.81 (*m*, 2H), 7.59–7.65 (*br*, 2H, *NH*×2), 5.56 and 5.08 (*br*, 2H, THP), 5.26 (*m*, 2H, *CHCH*₃×2), 4.08 and

SCHEME 3: Synthesis of Ruthenium Complexes Ru-3, Ru-4, and Ru-5


3.66 (m, 4H, THP), 3.46 and 3.40 (s, 6H, $\text{NCH}_3 \times 2$), 2.28–1.66 (br, 12H, THP), 1.55 (m, 6H, $\text{CHCH}_3 \times 2$).

The **Phen-2** was obtained from **Phen-1** after removal of the THP protecting group by heating for 2 h at 60 °C in an AcOH/ H_2O /THF (2:1:1) solution.⁴³ It was obtained in quantitative yield.

¹H NMR (250 MHz, CDCl_3) δ = 9.12 (s, 2H), 8.48 (m, 2H, $\text{NH} \times 2$), 7.95 (d, 2H, J = 8.1 Hz), 7.69 (d, 2H, 8.1 Hz), 7.55 (s, 2H), 5.34 (m, 2H, $\text{CHCH}_3 \times 2$), 3.33 (s, 6H, $\text{NCH}_3 \times 2$), 1.56 (d, 6H, J = 7 Hz). MS-ES $[\text{M} + \text{Na}]^+ = 489.5$.

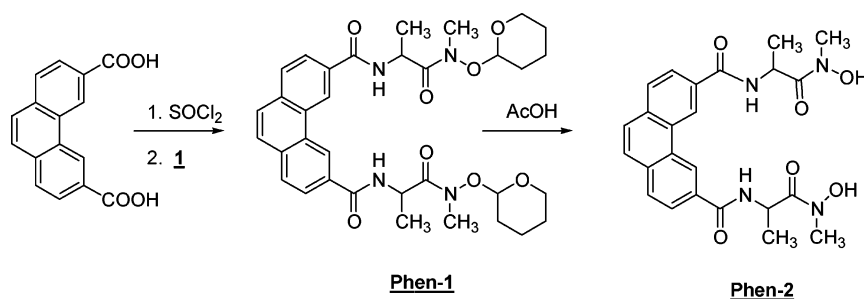
Ru-3, Ru-4, and Ru-5 (4–6) were prepared by coupling the corresponding amino derivatives with 2,2'-bipyridyl-4,4'-dicarboxylic acid chlorides.³²

Compound **4** was purified by column chromatography with MeOH/ CHCl_3 (4:96) as eluent and was obtained (124 mg, 0.318 mmol) in 24% yield.

¹H NMR (250 MHz, $\text{CDCl}_3/\text{MeOH}-d_4$) δ = 8.72 (dd, J = 5 and 0.6 Hz, 2H, bipy 5,5'), 8.62 (d, J = 0.6 Hz, 2H, bipy 3,3'), 7.97–8.00 (m, 2H, $\text{NH} \times 2$), 7.75 (dd, J = 5 and 1.7 Hz, 2H, bipy 3,3'), 4.69–4.75 (m, 2H, $\text{CHCH}_3 \times 2$), 3.73 (s, 6H, $\text{OCH}_3 \times 2$), 1.50 (d, J = 6.5 Hz, 6H, $\text{CHCH}_3 \times 2$).

Compound **5** was purified by column chromatography with MeOH/ CHCl_3 (6:94) as eluent and was obtained (300 mg, 0.602 mmol) in 98% yield.

¹H NMR (250 MHz, CDCl_3) δ = 8.77 (dd, J = 5 and 0.6 Hz, 2H, bipy 5,5'), 8.67 (m, 2H, bipy 3,3'), 7.74 (dd, J = 5 and 1.7 Hz, 2H, bipy 3,3'), 7.24–7.27 (m, 2H, $\text{NH} \times 2$), 4.65–4.77 (m, 2H, $\text{CHCH}_3 \times 2$), 1.50 and 1.53 (ov, 24H, $\text{CHCH}_3 \times 2$ and $\text{C}(\text{CH}_3)_3 \times 2$).

SCHEME 4: Synthesis of Phen-2


Compound **6** was purified by column chromatography with MeOH/ CHCl_3 (5:95) as eluent and was obtained (290 mg, 0.58 mmol) in quantitative yield.

¹H NMR (250 MHz, CDCl_3) δ = 8.77 (dd, J = 5 and 0.7 Hz, 2H, bipy 5,5'), 8.67 (m, 2H, bipy 3,3'), 7.74 (dd, J = 5 and 1.7 Hz, 2H, bipy 3,3'), 7.13 (m, 2H, $\text{NH} \times 2$), 3.73 (dt, J = 6 Hz and 6 Hz, 4H, $\text{NHCH}_2\text{CH}_2 \times 2$), 2.60 (t, J = 6 Hz, 4H, $\text{NHCH}_2\text{CH}_2 \times 2$), 1.48 (s, 18H, $\text{C}(\text{CH}_3)_3 \times 2$).

The ruthenium complexes were obtained by stirring the 2, 2'-bipyridyl derivatives **4–6** with equivalent amount of $\text{Ru}(\text{bipy})_2\text{Cl}_2 \cdot 6\text{H}_2\text{O}$ in 80% ethanolic solution for 4 h under argon followed by removal of the solvent and purification by column chromatography eluting with a $\text{CH}_3\text{CN}/n\text{-BuOH}/0.4 \text{ M KNO}_3$ (9:0.5:0.5) solution.

The butyl ester groups were removed by stirring in TFA/DCM (1:4) solutions for 1–2 h followed by evaporation of the solvents. **Ru-4** and **Ru-5** were obtained in quantitative yields. Complex **Ru-3** (40 mg, 0.042 mmol) was obtained in 38% yield.

Ru-3. ¹H NMR (250 MHz, MeOH- d_4) δ = 9.21 (s, 2H, s-bipy 3,3'), 8.73 (d, J = 7.8 Hz, 4H, bipy 3,3'), 8.12–8.20 (m, 4H, bipy 4,4'), 8.02 (d, J = 5.8 Hz, 2H, s-bipy 5,5'), 7.82–7.91 (ov, 4H of bipy 6,6' and 2H of s-bipy 6,6'), 7.48 (m, 4H, bipy 5,5'), 4.62–4.71 (m, 2H, $\text{CHCH}_3 \times 2$), 3.75 (s, 6H, $\text{OCH}_3 \times 2$), 1.55 (d, J = 7.4 Hz, 6H, $\text{CHCH}_3 \times 2$).

Ru-4. ¹H NMR (250 MHz, MeOH- d_4) δ = 9.19 (s, 2H, s-bipy 3,3'), 8.73 (d, J = 8.2 Hz, 4H, bipy 3,3'), 8.11–8.19 (m, 4H, bipy 4,4'), 8.01 (d, J = 5.8 Hz, 2H, s-bipy 5,5'), 7.81–7.89 (ov, 4H of bipy 6,6' and 2H of s-bipy 6,6'), 7.46–7.54 (m, 4H, bipy 5,5'), 4.59–4.68 (m, 2H, $\text{CHCH}_3 \times 2$), 1.56 (d, J = 7.3 Hz, 6H, $\text{CHCH}_3 \times 2$).

Ru-5. ¹H NMR (250 MHz, MeOH- d_4) δ = 9.10 (s, 2H, s-bipy 3,3'), 8.71 (d, J = 8.0 Hz, 4H, bipy 3,3'), 8.10–8.18 (m, 4H, bipy 4,4'), 7.98 (d, J = 6.0 Hz, 2H, s-bipy 5,5'), 7.79–7.83 (ov, 6H, bipy 6,6' and s-bipy 6,6'), 7.44–7.53 (m, 4H, bipy 5,5'), 3.67 (t, J = 6.6 Hz, 4H, $\text{NHCH}_2\text{CH}_2 \times 2$), 2.65 (t, J = 6.6 Hz, 4H, $\text{NHCH}_2\text{CH}_2 \times 2$).

Results and Discussion

1. Synthesis. *Ru-1.* The metal complex, **Ru-1**, and all other ruthenium complexes in this study were prepared according to Schemes 2 and 3. The synthesis of the organic analogue (**Phen-2**) is shown in Scheme 4.

2. How Does the Hydroxamic Acid Contribute to the Stability of the Cage Complex? *Comparison between Ru-1 and Ru-2.* Irradiation of **Ru-1** and **Ru-2** in $\text{CH}_3\text{CN}/\text{H}_2\text{O}$ solutions by visible light ($\lambda_{\text{max}} = 450 \text{ nm}$) leads to the formation of radicals with a g factor of 2.0061 (Figure 2). The 12-line EPR signal, corresponding to the nitroxyl radical ($a_{\text{N}} = 6.83 \text{ G}$ and $a_{\text{H}} = 7.87 \text{ G}$), is similar to that observed for the radical of *N*-methyl-*N*-acetyl-hydroxylamine.⁴⁴

The kinetics of the radical formation was found to be very modest, resulting from oxidation of the hydroxamic acid group

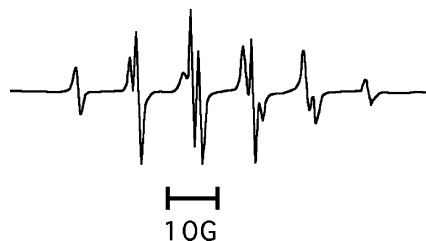


Figure 2. EPR spectrum of the nitroxyl radical formed on irradiation of **Ru-1** and **Ru-2**.

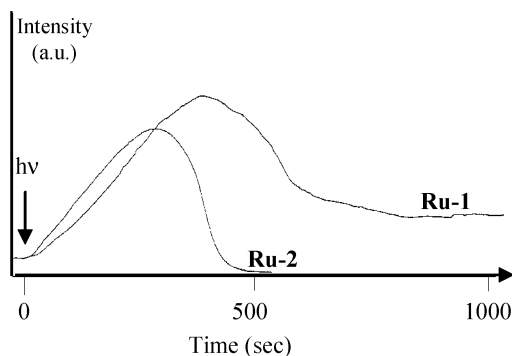


Figure 3. Formation of nitroxyl radicals in 1 mM solutions of **Ru-1** and **Ru-2** in the presence of 50 mM PBN. The EPR signal was fixed at 3273 G (doublet) and recorded with a receiver gain of 8×10^4 and modulation amplitude of 1 G.

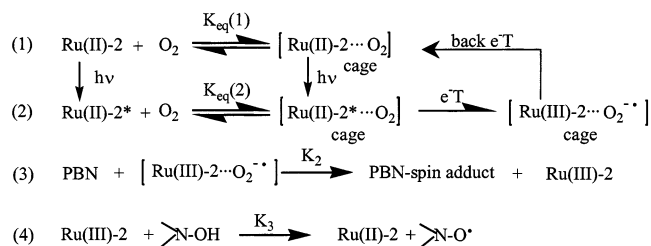
by singlet oxygen, produced by energy transfer from Ru(II)^* to molecular oxygen.³² Irradiating the solution of **Ru-2** in the presence of a spin trap, that is, PBN and DMPO, revealed a dramatic enhancement in the concentration of nitroxyl radicals (up to 30 times). Addition of superoxide dismutase also stimulated the generation of nitroxyl radical, but less extensively than spin traps.³² Removal of oxygen by argon bubbling inhibited nitroxyl radical formation.³²

This observation was attributed to the high reactivity of Ru(III) ions, with a high redox potential $\{E_0(\text{Ru}^{2+/3+}) = 1.29 \text{ V}\}$,^{45,46} which is responsible for the formation of the nitroxyl radicals. The Ru(III) ion, produced in the irradiated solution, is trapped in a cage complex with a superoxide radical $[\text{Ru(III)} \cdots \text{O}_2^{\cdot-}]$. A reverse electron-transfer reaction, $\text{Ru(III)} + \text{O}_2^{\cdot-} \rightarrow \text{Ru(II)} + \text{O}_2$, could play a role in the equilibrium. The spin traps liberate the superoxide radical from the cage complex and facilitate further reaction of Ru(III) with the hydroxamic acid (See Scheme 1A).

To evaluate the effect of the two hydroxamic acid groups on stability of the proposed cage complex, a second ruthenium complex (**Ru-1**), with a single hydroxamic acid group on the bipyridyl ring, was synthesized (Scheme 2). It was expected that a weaker cage would be obtained with this derivative and that the effect of the spin trap would be less pronounced. From the EPR study, it was clear that for both complexes (**Ru-2** and **Ru-1**) the formation of the nitroxyl radical was accelerated by spin trap molecules. However, the formation rate of the nitroxyl radical was faster in **Ru-2** than in **Ru-1** solution (Figure 3). Nitroxyl radical concentration decreases after several minutes of irradiation of both compounds, probably because of the light-induced photooxidation of the nitroxyl radical to the diamagnetic *N*-oxo-ammonium ion by Ru(III) .⁴⁷

The proposed reaction mechanism is described in Scheme 5, where $K_{\text{eq}}(1) = K_{\text{eq}}(2) = K_1/K_{-1}$, assuming that the complex in its excited state has the same affinity for O_2 as in its ground state.

SCHEME 5: Light-Dependent Mechanisms for the Generation of Nitroxyl Radicals in the Presence of PBN



3. Spectroscopic Evidence Supporting Cage Formation with Molecular Oxygen. *3a. EPR Kinetics of Nitroxyl Radical Formation as a Function of Temperature.* As can be seen from the system of eqs 1–4 describing the kinetics of nitroxyl radical generation under photoexcitation of our **Ru(II)-2** complex, there are a few temperature-dependent steps.

The effect of temperature on the direct and back electron-transfer reactions requires a separate consideration. The electron-transfer rate K in our system is described by the Marcus formula:⁴⁸

$$\ln(K/K_0) = (\Delta G_i + \lambda)^2 / 4\lambda kT \quad (5)$$

where ΔG_i is the Gibbs free-energy change in the overall electron transfer (e^-T) reaction and λ is the reorganization energy. For known Ru complexes, the electron-transfer reaction between Ru(II)^* and O_2 has $\Delta G(e^-T)$ ranging from -0.04 to -0.72 eV .²⁹ On the other hand, $\Delta G_{\text{back}}(e^-T)$ is in the range of -1.78 to -2.46 eV (for estimation of $\Delta G_{\text{back}}(e^-T)$ we used an energy of light for excitation of our **Ru(II)-2** = 2.5 eV). From the classical parabolic Marcus dependence of $\ln K$ versus ΔG_i (see, for example, refs 48 and 49), it follows that the rate of direct electron-transfer reaction is 10^2 to 10^3 orders of magnitude higher than the back electron-transfer reaction, which means that the reaction shifts significantly to the right side (see Scheme 5, eqs 1 and 2).

The bimolecular reaction between the ‘trapped’ superoxide radical and PBN (Scheme 5, eq 3) is expected to speed up with temperature and to be accompanied by an increase in concentration of nitroxyl radicals.⁵⁰ However, taking into account temperature dependence of electron transfer and back electron-transfer reactions, such behavior should describe a system where no equilibria between **Ru(II)-2** and O_2 are formed (eqs 1 and 2). When these equilibria and cage complexes are involved, elevation of temperature is expected to cause a decrease in K_{eq} . As a result, concentrations of ‘bound’ oxygen, superoxide radicals, and Ru(III) ions should decrease together with the concentration of nitroxyl radicals.

The EPR spectra of ruthenium complexes **Ru-2** and **Ru-1** were recorded at different temperatures in the presence (Figure 4) and in the absence (Figure 5) of the spin trap PBN. The decrease in the initial rate of formation of the nitroxyl radicals with increasing temperature for both complexes supports the existence of cage complexes (Figure 4).

Oxygen solubility, as with other gases, decreases with increasing temperature.⁵¹ For the known values of oxygen concentration within the temperature range under study, a maximum effect could be 1.27. At the same time, an experimentally observed decrease of nitroxyl radical generation rate was 1.72–2. Note that an increase in $^1\text{O}_2$ generation rate (Figure 5) with increasing temperature (and decreasing O_2 concentration in solution!) also indicates that concentration of oxygen is insignificant for the kinetic behavior observed (Figure 4).

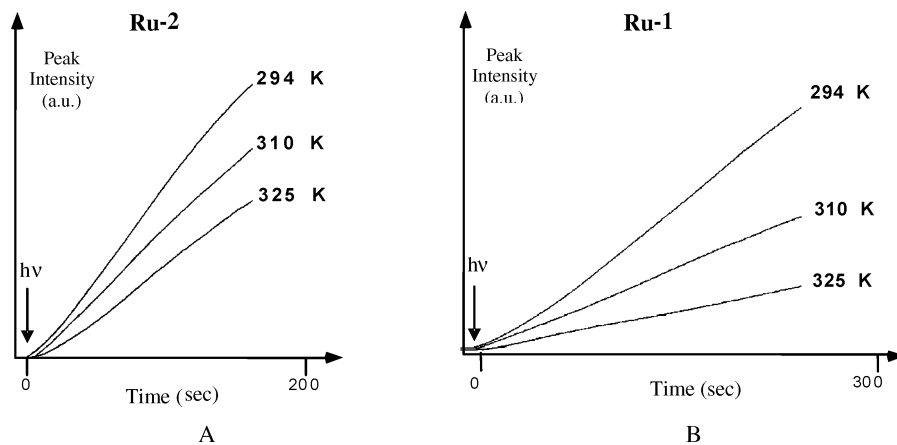


Figure 4. Effect of temperature on the rate of nitroxyl radical formation in 1 mM solutions of **Ru-2** (A) and of **Ru-1** (B) in the presence of 50 mM PBN. The EPR signal was fixed at 3170.1 G (triplet) and recorded with a receiver gain of 5×10^4 and a modulation amplitude of 2.2 G.

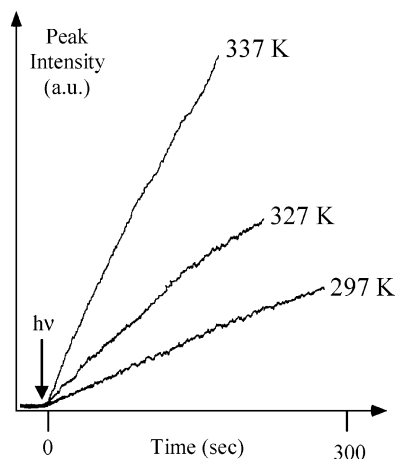


Figure 5. Effect of temperature on the rate of nitroxyl radical formation in a 1 mM solution of **Ru-2**. The EPR signal was fixed at 3164.3 G (doublet) and recorded with a receiver gain of 4×10^5 and a modulation amplitude of 2.0 G.

In the absence of spin traps, the nitroxyl radicals result from collisions between molecules of singlet oxygen (formed via energy transfer from Ru(II)^* to molecular oxygen (Scheme 1B)) and the hydroxamic acid group. Since in this type of bimolecular reaction the collisions between the singlet oxygen molecule and the hydroxamic acid are essential, raising the temperature should increase the reaction rate. This type of reactivity was indeed observed when a solution of **Ru-2** was irradiated at elevated temperatures (Figure 5).

3b. Effect of Oxygen on the Chemical Shifts of Specific Protons in the ^1H NMR Spectra of **Ru-2 and **Ru-1**.** Molecular oxygen is a paramagnetic molecule and therefore is expected to induce paramagnetic shifts in the NMR signals of 'magnetically active' atoms and ions that are in its close vicinity. Recently, O_2 has been used as a shift reagent in solid state NMR spectroscopy to probe accessibility of caption sites in zeolites.^{52–56} Also, O_2 has been successfully applied as a paramagnetic reporter of membrane protein topology, since it is inhomogeneously distributed in biological membranes and thus gives rise to an exquisite range of position-dependent paramagnetic effects.³⁵ We have used this property to confirm the existence of a cage structure between **Ru-2** and the oxygen molecule in acetonitrile by recording the ^1H NMR spectra of the complex in oxygen, air, and argon atmospheres. We expected to observe changes in the chemical shifts for those protons that are in close contact with the O_2 molecule trapped in the cage. It is important to emphasize that if interactions between **Ru-2** and the oxygen

molecules are based only on collisions, nonselective shifts will occur. In fact, we have observed a downfield shift of $\Delta\delta = 5.6$ Hz of only two protons attached to one of the bipyridyl ligands (i.e., the peaks of the protons at positions 3 and 3' (Figure 6)). Similar behavior was observed in the ^1H NMR spectrum of **Os-2** in the presence of O_2 (data not shown).

To assess whether both hydroxamic acid groups are required for the formation of the cage, we have looked for the formation of a cage between **Ru-1** and O_2 by performing a similar NMR experiment. A less pronounced downfield shift of $\Delta\delta = 1.6$ Hz for H_3 (Figure 7A) and no shift at all for H_3' were obtained for the system with only one hydroxamic acid attached to the bipyridyl ring. (Figure 7B)

The conclusion from the experiment is that though a cage is formed when only one hydroxamic acid is present, both hydroxamic acid groups are required for the formation of a stable cage with oxygen.

A series of model complexes (**Ru-3**, **Ru-4**, and **Ru-5**) in which the side chains are terminated with carboxylic acid (**Ru-4** and **Ru-5**) or ester (**Ru-3**) functional group was prepared. The length of the side chain was also extended by replacing an L-alanine amino acid (**Ru-4**) with a β -alanine (**Ru-5**). In all cases, no shifts in the peaks of the protons in the 3, 3'-bipyridyl positions were observed in the ^1H NMR spectra in the presence of oxygen, indicating no detectable affinity for O_2 . Other model compounds that lack a metal center, including a free ligand and a phenanthroline derivative (**Phen-2**) with two hydroxamic acid groups attached to its skeleton with a similar mutual orientation as in **Ru-2**, were also prepared and studied. No shifts in the ^1H NMR spectra of these compounds were observed in the presence of O_2 . These observations imply that the metal (Ru(II) or Os(II)) and the hydroxamic acid group are essential prerequisites for cage formation.

We want to emphasize that the paramagnetic shift effects of oxygen depend on the lifetime of the complex. For zeolites, where the oxygen is absorbed within the cavities, the effect was achieved by increasing the oxygen concentration and decreasing the sample's temperature.^{52–56} The selective low field shifts of the 3, 3' protons in **Ru-2** are related to the relatively long lifetime of the 'caged' oxygen. According to our knowledge, the cage described in the present work is the first observation of a complex between a metal complex and molecular oxygen that is not chemically coordinated via the metal center, in solution at room temperature.

3c. Estimation of K_{eq} for $\text{Ru(II)} + \text{O}_2 \rightleftharpoons \text{Ru(II)}-\text{O}_2$. The EPR and NMR data indicate that **Ru-2** can produce a complex with molecular oxygen and the superoxide radical. To estimate the

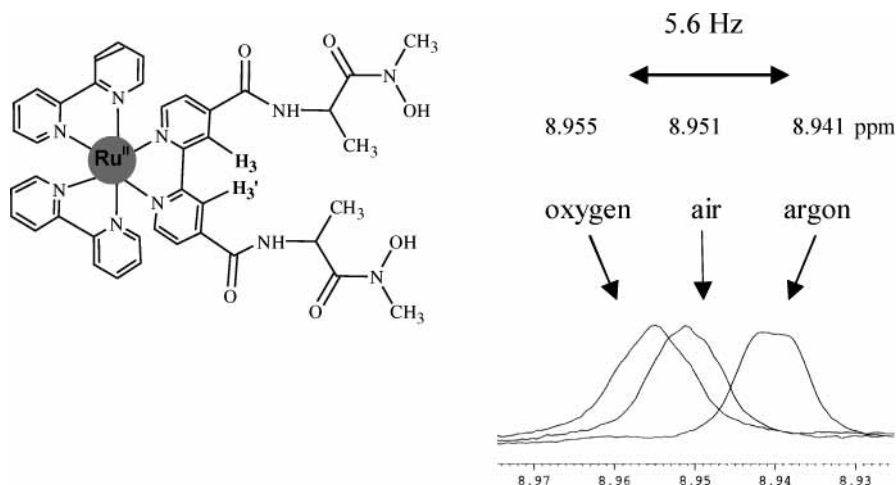


Figure 6. Peaks of protons 3 and 3' in the ^1H NMR spectrum of **Ru-2** in O_2 , air, and argon atmospheres. The sample was dissolved in CD_3CN and the spectrum was recorded at 400 MHz.

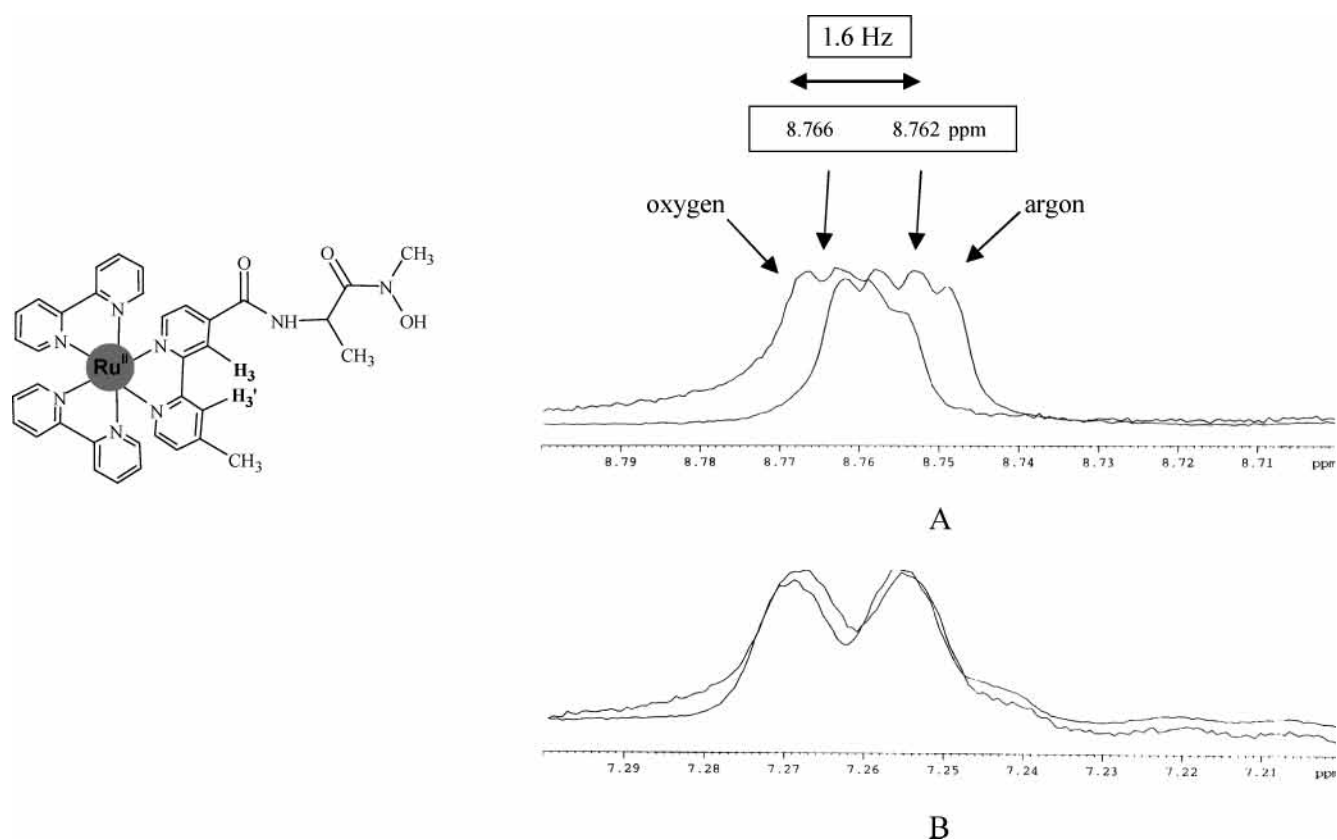


Figure 7. Peaks of protons 3 (A) and 3' (B) in the ^1H NMR spectrum of **Ru-1** in O_2 , air, and argon atmospheres, respectively. The sample was dissolved in CD_3CN and the spectrum was recorded at 400 MHz.

equilibrium constant for **Ru-2** with molecular oxygen, we measured the rates of nitroxyl radical production for different concentrations of ruthenium complex (see Figure 8). It is clearly seen (see Figure 9) that dR/dt (rate of nitroxyl radical generation) as a function of **Ru-2** concentration follows eq 6:

$$\tan \alpha = K_2 \times K_{\text{eq}}(2) \times [\text{O}_2]_0 \times [\text{PBN}] \quad (6)$$

Here, K_2 is a bimolecular rate constant between the cage complex and PBN, $K_{\text{eq}}(2)$ is the equilibrium constant for **Ru-2** and molecular oxygen, $[\text{O}_2]_0$ is the concentration of molecular oxygen in solution (in our case ~ 0.5 mM), and $[\text{PBN}]$ is the concentration of the spin trap in solution (0.05 M).

Greenstock et al.⁵⁰ have estimated the bimolecular rate constant for the reaction of PBN with $\text{O}_2^{\bullet-}$ to be smaller than

$10^6 \text{ M}^{-1} \text{ s}^{-1}$, and the reaction rate of $\text{O}_2^{\bullet-}$ with DMPO was calculated as $K_2 = 10 \text{ M}^{-1} \text{ s}^{-1}$ (see ref 57). We used this value in our calculations as the K_2 value for the reaction of PBN and superoxide, as there is no published value for PBN. As all other parameters in eq 6 are known, we have inserted them in the equation and estimated the value of K_{eq} to be 3.1 M^{-1} . A detailed calculation of K_{eq} is available as Supporting Information.

4. Comparing the Photoinduced Processes in Ru-2 and in Os-2. The similarity between Ru(II) and Os(II) in photochemical behavior and redox properties led us to compare osmium to ruthenium complexes. The Os(II) tris-polypyridyl complexes have similar redox potentials to those of the Ru(II) complexes, but their excited-state lifetime is shorter.^{58,59} Therefore, it was expected that the energy and electron-transfer

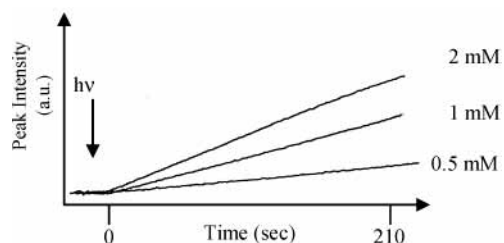


Figure 8. Rates of nitroxyl radical formation of **Ru-2** in the presence of 50 mM PBN for different concentrations of the complex. The EPR signal was fixed at 3272.1 G (doublet) and recorded with a receiver gain of 5×10^4 and modulation amplitude of 1.0 G.

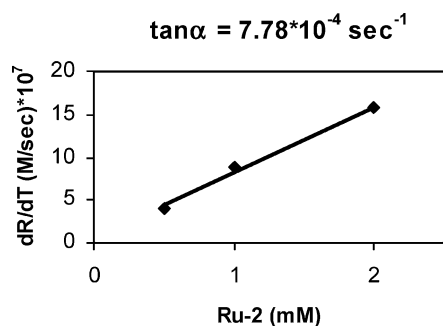


Figure 9. Calculation of K_{eq} from the **Ru-2** concentration dependence on nitroxyl radical formation.

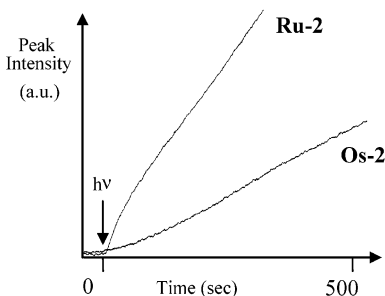


Figure 10. Rate of nitroxyl radical formation in 2 mM solutions of **Os-2** and **Ru-2**. The EPR signal was fixed at 3182.2 G (doublet) and recorded with a receiver gain of 4×10^5 and a modulation amplitude of 1.0 G.

processes would be less effective for Os(II) than for Ru(II) complexes.

In fact, irradiation of **Os-2** leads to the formation of the nitroxyl radicals, with a similar EPR spectrum to that shown in Figure 2. A comparison of the kinetics of nitroxyl radicals formation in **Os-2** and **Ru-2** solutions shows that the **Os-2** is less effective than **Ru-2**. (Figure 10).

The effect of PBN on the rate of formation of nitroxyl radical in **Os-2** was also very modest (Figure 11) and less pronounced than that observed for **Ru-2** (Figure 12), which is in agreement with the shorter lifetime of the Os excited state. In addition, one cannot rule out the possibility that the geometry of **Os-2** is less favorable for binding molecular oxygen as compared to that of **Ru-2** or that there are other photophysical reasons for the differences observed. Of crucial importance for us is the fact that different photoactive metal complexes can produce long-lived complexes (cage) with molecular oxygen.

Conclusions

In this study, we present EPR data that suggests the formation of a cage complex between the superoxide radical and **Ru-2** and a less stable cage with **Ru-1**, where a single hydroxamic acid group is attached to one of the bipyridyl ligands.

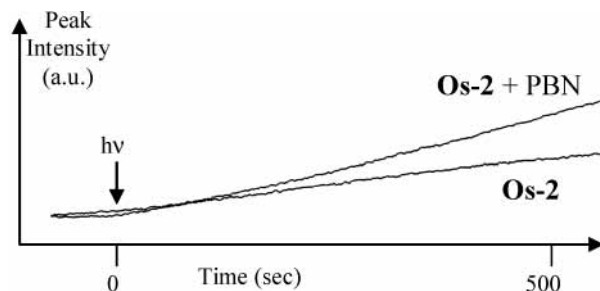


Figure 11. Rate of nitroxyl radical formation in solutions (1 mM) of **Os-2** with/without PBN (50 mM). The EPR signal was fixed at 3182.2 G (doublet) and recorded with a receiver gain of 2×10^5 and a modulation amplitude of 1.0 G.

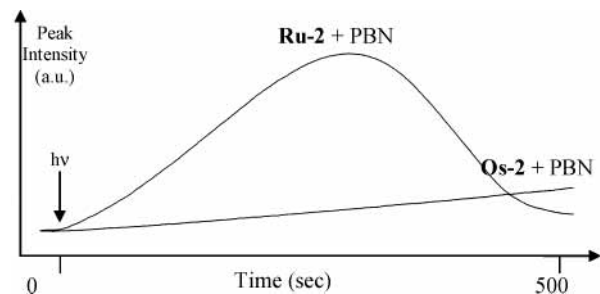


Figure 12. Rate of nitroxyl radical formation in solutions (1 mM) of **Os-2** and **Ru-2** in the presence of PBN (50 mM). The EPR signal was fixed at 3182.2 G (doublet) and recorded with a receiver gain of 8×10^4 and a modulation amplitude of 1.0 G.

In an attempt to trace the origin of this unique behavior, we prepared a series of model compounds and studied them in the presence and absence of molecular oxygen.

The NMR data indicate that carboxylic acids in the **Ru-4** and **Ru-5** compounds are not effective in forming the cage complex with molecular oxygen. This may result from the tendency of carboxylic acids (in close proximity) to readily form intramolecular hydrogen bonding, thereby excluding their binding to O_2 .

To our surprise, the organic analogue (**Phen-2**), whose ligand structure is similar to that of **Ru-2**, had no detectable affinity for O_2 . This may be related to subtle differences in the aromatic ring geometry. We believe, however, that the most likely reason is stabilization of the cage complex by the positive metal ion center that does not exist in this organic analogue. The detailed nature of these interactions is not completely clear. Research in this direction is under way.

Thus, using NMR we were able to show that the origin of a unique behavior of ruthenium and osmium hydroxamate complexes could be attributed to their ability to interact with free oxygen, even in the ground state (triplet state). As a result, a genuine cage complex can be formed upon irradiation.

Acknowledgment. The authors thank Dr. Leonid Konstantinovski for his helpful advice in conducting NMR experiments and Prof. Anatoly Burshtein for useful discussions. Support from the Helen and Martin Kimmel Center for Molecular Design is greatly acknowledged. A.S. holds the Siegfried and Irma Ulmann professorial chair.

Supporting Information Available: A detailed calculation of K_{eq} for cage formation. This material is available free of charge via the Internet at <http://pubs.acs.org>.

References and Notes

- (1) Gilbert, J. A.; Eggleston, D. S.; Murphy, W. R. J.; Geselowitz, D. A.; Gersten, S. W.; Hodgson, D. J.; Meyer, T. J. *J. Am. Chem. Soc.* **1985**, *107*, 3855.

- (2) Ghosh, P. K.; Brunshwig, B. S.; Chou, M.; Creutz, C.; Sutin, N. *J. Am. Chem. Soc.* **1984**, *106*, 4772.
- (3) Shiroishi, H.; Nukaga, M.; Yamashita, S.; Kaneko, M. *Chem. Lett.* **2002**, *4*, 488.
- (4) Shiroishi, H.; Yamashita, S.; Kaneko, M. *J. Mol. Catal. A: Chem.* **2001**, *169*, 269.
- (5) Morris, N. D.; Mallouk, T. E. *J. Am. Chem. Soc.* **2002**, *124*, 11114.
- (6) Yamada, H.; Koike, T.; Hurst, J. K. *J. Am. Chem. Soc.* **2001**, 12775.
- (7) Amouyal, E. *Sol. Energy Mater. Sol. Cells* **1995**, *38*, 249.
- (8) Wagenknecht, H. A.; Stemp, E. D. A.; Barton, J. K. *J. Am. Chem. Soc.* **2000**, *122*, 1.
- (9) Ortmans, I.; Content, S.; Buotonnet, N.; Mesmaeker, A. K.-D.; Bannawarth, W.; Constant, J.-F.; Defranco, E.; Lhomme, J. *Chem.—Eur. J.* **1999**, *5*, 2712.
- (10) Carter, P. J.; Cheng, C.-C.; Thorp, H. H. *J. Am. Chem. Soc.* **1998**, *120*, 632.
- (11) O'Reilly, F.; Kelly, J.; Mesmaeker, A. K. *Chem. Commun.* **1996**, 1013.
- (12) Tossi, A. B.; Kelly, J. M. *Photochem. Photobiol.* **1989**, *49*, 545.
- (13) Farrer, B. T.; Thorp, H. H. *Inorg. Chem.* **2000**, *39*, 44.
- (14) Araki, K.; Silva, C. A.; Toma, H. E.; Catalani, L. H.; Medeiros, M. H. G.; Di Mascio, P. *J. Inorg. Biochem.* **2000**, *78*, 269.
- (15) Nunez, M. E.; Barton, J. K. *Curr. Opin. Chem. Biol.* **2000**, *4*, 199.
- (16) Hamachi, I.; Tsukiji, S.; Shinkai, S.; Oishi, S. *J. Am. Chem. Soc.* **1999**, *121*, 5500.
- (17) Wilker, J. J.; Dmochowski, I. J.; Dawson, J. H.; Winkler, J. R.; Gray, H. B. *Angew. Chem., Int. Ed. Engl.* **1999**, *38*, 90.
- (18) Liu, R. Q.; Hahn, S.; Miller, M.; Durham, B.; Millett, F. *Biochem.* **1995**, *34*, 973.
- (19) Murphy, C. J.; Arkin, M. R.; Ghatlia, N. D.; Bossmann, S.; Turro, N. J.; Barton, J. K. *Proc. Natl. Acad. Sci. U.S.A.* **1994**, *91*, 5315.
- (20) Margalit, R.; Kostic, N. M.; Che, C. M.; Blair, D. F.; Chiang, H. J.; Pecht, I.; Shelton, J. B.; Shelton, J. R.; Schroeder, W. A.; Gray, H. B. *Proc. Natl. Acad. Sci. U.S.A.* **1984**, *81*, 6554.
- (21) Aoudia, M.; Guliaev, A. B.; Leontis, N. B.; Rodgers, M. A. J. *Biophys. Chem.* **2000**, *83*, 121.
- (22) Fancy, D. A.; Denison, C.; Kim, K.; Xie, Y.; Holdeman, T.; Amini, F.; Kodadek, T. *Chem. Biol.* **2000**, *7*, 697.
- (23) Bishop, B. M.; McCafferty, D. G.; Erickson, B. W. *Tetrahedron* **2000**, *56*, 4629.
- (24) Stemp, E. D. A.; Holmlin, R. E.; Barton, J. K. *Inorg. Chim. Acta* **2000**, *297*, 88.
- (25) Dunn, A. R.; Dmochowski, I. J.; Winkler, J. R.; Gray, H. B. *J. Am. Chem. Soc.* **2003**, *125*, 12450.
- (26) Contakes, S. M.; Dunn, A. R.; Morales, N.; Winkler, J. R.; Gray, H. B. *J. Inorg. Biochem.* **2003**, *96*, 120.
- (27) Gross, Z.; Mahammed, A.; Abdalles, M.; Weaver, J. J.; Gray, H. B. *J. Inorg. Biochem.* **2003**, *96*, 140.
- (28) Di Bilio, A. J.; Crane, B. R.; Wehbi, W. A.; Kiser, C. N.; Abu-Omar, M. M.; Carlos, R. M.; Richards, J. H.; Winkler, J. R.; Gray, H. B. *J. Am. Chem. Soc.* **2001**, *123*, 3181.
- (29) Zhang, X.; Rodgers, M. A. J. *J. Phys. Chem.* **1995**, *99*, 12797.
- (30) Davies, M. J.; Donkor, R.; Dunster, C. A.; Gee, C. A.; Jonas, S.; Willson, R. L. *Biochem. J.* **1987**, *246*, 725.
- (31) Morehouse, K. M.; Flitter, W. D.; Mason, R. P. *FEBS Lett.* **1987**, *222*, 246.
- (32) Yavin, E.; Weiner, L.; Arad-Yellin, R.; Shanzer, A. *J. Phys. Chem. A* **2001**, *105*, 8018.
- (33) La Mar, G. N.; Budd, D. L.; Sick, H.; Gersonde, K. *Biochim. Biophys. Acta* **1978**, *537*, 270.
- (34) Barrette, W. C.; Johnson, H. W.; Sawyer, D. T. *Anal. Chem.* **1984**, *56*, 1890.
- (35) Luchette, P. A.; Prosser, R. S.; Sanders, C. R. *J. Am. Chem. Soc.* **2002**, *124*, 1778.
- (36) McCafferty, D. G.; Bishop, B. M.; Wall, C. G.; Hughes, S. G.; Mecklenberg, S. L.; Meyer, T. J.; Erickson, B. W. *Tetrahedron* **1995**, *51*, 1093.
- (37) Nakonieczna, L.; Chimiak, A. *Synthesis* **1987**, 418.
- (38) Kober, E. M.; Caspar, J. V.; Sullivan, B. P.; Meyer, T. J. *Inorg. Chem.* **1988**, *27*, 4587.
- (39) Hirai, Y.; Aida, T.; Inoue, S. *J. Am. Chem. Soc.* **1989**, *111*, 3062.
- (40) Langer, M. E.; Khorshahi, F. *Process for preparation of 4,4'-stilbenedicarboxylates by Wittig reaction of 4-(halomethyl)benzoate with 4-formylbenzoate*; Lever Brothers Co.: 1992.
- (41) Rosa, J. C.; Galanakis, D.; Ganellin, C. R.; Dunn, P. M. *J. Med. Chem.* **1996**, *39*, 4247.
- (42) Khalaf, A. I.; Pitt, A. R.; Scobie, M.; Suckling, C. J.; Urwin, J.; Waigh, R. D.; Fishleigh, R. V.; Young, S. C.; Wylie, W. A. *Tetrahedron* **2000**, *56*, 5225.
- (43) Bernady, K. F.; Floyd, M. B.; Poletto, J. F.; Weiss, M. J. *J. Org. Chem.* **1979**, *44*, 1438.
- (44) Green, E. S. R.; Evans, H.; Rice-Evans, P.; Davies, M. J.; Salah, N.; Rice-Evans, C. *Biochem. Pharmacol.* **1993**, *45*, 357.
- (45) Kalyanasundaram, K. *Coord. Chem. Rev.* **1982**, *46*, 159.
- (46) Erkkila, K. E.; Odom, D. T.; Barton, J. K. *Chem. Rev.* **1999**, *99*, 2777.
- (47) Ford, W. E.; Rodgers, M. A. J. *J. Phys. Chem. B* **1997**, *101*, 930.
- (48) Markus, R. A. P.; Siders, P. J. *J. Phys. Chem.* **1982**, *86*, 622–630.
- (49) Connolly, J. S.; Bolton, J. R. In *Photoinduced Electron Transfer, Part D*; Fox, M. A. Chanon, M., Eds.; Elsevier: 1988; Chapter 6.2.
- (50) Greenstock, C. L.; Wiebe, R. H. *Can. J. Chem.* **1982**, *60*, 1560.
- (51) Battino, R.; Clever, H. L. *Chem. Rev.* **1966**, *66*, 395–463.
- (52) Plevert, J.; de Menorval, L. C.; DiRenzo, F.; Fajula, F. *J. Phys. Chem. B* **1998**, *102*, 3412.
- (53) Accardi, R. J.; Lobo, R. F. *J. Phys. Chem. B* **2001**, *105*, 5883.
- (54) Feuerstein, M.; Accardi, R. J.; Lobo, R. F. *J. Phys. Chem. B* **2000**, *104*, 10282.
- (55) Liu, H.; Kao, H.-M.; Grey, C. P. *J. Phys. Chem. B* **1999**, *103*, 4786.
- (56) Liu, H.; Grey, C. P. *Microporous Mesoporous Mater.* **2002**, *53*, 109.
- (57) Finkelstein, E.; Rosen, G. M.; Rauckman, E. J. *J. Am. Chem. Soc.* **1980**, *102*, 4994.
- (58) Hauenstein, B. L.; Dressick, W. J.; Buell, S. L.; Demas, J. N.; DeGraff, B. A. *J. Am. Chem. Soc.* **1983**, *105*, 4251.
- (59) Sutin, N.; Cruetz, C. *Pure Appl. Chem.* **1980**, *52*, 2717.